522

Reprinted from
"Proceedings of the Fifth Carbon Conference"
Volume II

PERGAMON PRESS

OXFORD · LONDON · NEW YORK · PARIS

1963

Printed in Great Britain by J. W. Arrowsmith Ltd., Bristol 3

Reprinted Author

1

MODE OF POROSITY DEVELOPMENT IN ACTIVATED ANTHRACITE[1]

M. KAWAHATA and P. L. WALKER, JR.
Department of Fuel Technology, The Pennsylvania State University, University Park, Pennsylvania

(Manuscript received September 20, 1961)

A St. Nicholas anthracite was devolatilized at 950°C and then activated with CO_2 at temperatures between 800° and 950°C in a fluidized reactor with the extent of burnoff ranging from 8 to 65%[2]. Three particle sizes in the range from 16 × 20 to 100 × 150 mesh (Tyler) were employed. To characterize the pore structure of the activated anthracite, surface area, helium density, apparent density, and pore volume distribution data were obtained. As the activation progressed up to 65% burnoff at 900°C, the specific surface area and pore volume increased to 2120 m^2/g and 0.79 cm^3/g, respectively for the 100 × 150 mesh size. These values are the maximum obtained for all of the activation conditions used. The pore volume distribution of the activated anthracite can be expressed by a normal distribution function having three sets of parameters, taking the logarithm of pore diameter as the independent variable. For all samples, the first distribution function covers the volume of pores smaller than 30 Å in diameter and it comprises about 92% of the total pore volume. Development of the fine pore structure involves a two-fold process consisting of (1) opening of pores originally closed and (2) enlargement of open pores. The first process predominates at the initial stages of burnoff, while the second process becomes of importance at higher burnoffs. The rate of activation of anthracite with CO_2 over the temperature range studied is controlled jointly by the chemical rate and the rate of diffusion of CO_2 into the internal pore structure. Consequently, the development of micropores takes place less uniformly with increase in temperature and/or particle size.

I. INTRODUCTION

Activated carbons are produced by mild oxidation of chars produced from various carbonaceous materials such as lignite, bituminous coal, wood, and nutshells. The history and nature of the carbonaceous material as well as process conditions determine the properties of the activated carbon produced. It is generally accepted that activated carbons owe their high adsorptive capacities to an internal structure which consists of a large number of interconnecting, fine pores. This internal pore structure has been described by parameters such as pore volume, pore surface area, and pore volume distribution in order to better understand the adsorptive characteristics of activated carbons.

Anthracite has a considerable porosity, with a large fraction of the porosity in pore sizes of molecular dimensions[3–5]. Suitably treated, this fine pore structure of anthracite could be utilized for the successful production of activated carbons. Clendenin and coworkers[6] studied a process for the steam activation of various Pennsylvania anthracites, in which they varied temperature, amount of burnoff, steam flow rate, and anthracite particle size. They concluded that anthracite was a suitable raw material for the production of activated carbons.

[1] In part, based on a Ph.D. thesis submitted by M. Kawahata to the Graduate School of The Pennsylvania State University, January, 1960.

[2] Per cent burnoff and all of the pore structure data are based on a mineral matter free basis (m.f.b.).

[3] P. B. Hirsch, *Proc. Roy. Soc.* (*London*) **A226**, 143 (1954).

[4] R. L. Bond and D. H. T. Spencer, *Industrial Carbon and Graphite Conference*, London, p. 231 (1958).

[5] R. B. Anderson, W. K. Hall, J. A. Leeky, and K. C. Stein, *J. Phys. Chem.* **60**, 1548 (1956).

[6] J. D. Clendenin, W. T. Griffiths, and C. C. Wright, *Trans. Ann. Anthracite Conf.* **10**, 121, Lehigh University (1952).

Hassler [7,8] studied a process for producing activated carbons from anthracite using steam in a fluidized bed. At a weight loss of 20%, the activated anthracite had a surface area of about 800 m^2/g. In both of the above studies the pore structure of the product carbons was not thoroughly investigated.

Numerous papers have been published on the pore structure of activated carbons and on their adsorption characteristics for various adsorbates. However, the manufacturing process conditions used for activation of these carbons have not been available in the literature. It was decided, therefore, that in this research a systematic study of the effect of process conditions on the pore structure and adsorption characteristics of activated anthracites should be made.

The purpose of this research then was concerned with the following objectives:

(1) to investigate the effect of the process conditions on the pore structure of the activated anthracites and to clarify the mechanism of development of pore structure in anthracite as activation proceeds.

(2) to investigate the adsorptive characteristics of activated anthracites for organic vapors as a function of the process conditions and their pore structures.

(3) to evaluate activated anthracites by comparing their properties with activated carbons presently being marketed commercially.

This paper covers the initial stage of a systematic study, with the work being restricted to activation of one anthracite using CO_2 as the oxidizing gas. The findings pertinent to objective (1) are presented in this paper. The major results concerning objectives (2) and (3) are presented elsewhere[9].

II. EXPERIMENTAL

A. *Samples*

An anthracite from the St. Nicholas breaker of the Reading Anthracite Company was used for all the activation runs reported. The anthracite had a surface area of 1.5 m^2/g, as determined by N_2 adsorption at 78°K. The proximate analysis of this anthracite is shown in Table I.

TABLE I

Proximate Analysis of St. Nicholas Anthracite (as received)

Moisture	1.1%
Volatile matter	3.0
Ash	7.7
Fixed carbon	88.2

B. *Activation of Anthracite*

1. *Apparatus.* The activation apparatus is described in detail in a previous paper[9]. Essentially, it consisted of a preheater, a fluidized reactor, and a product gas-analysis system. The fluidized reactor was a Hastelloy-C tube 1.94 in. I.D. by 5 ft long. It was heated externally. The sample being activated was supported on a packed bed of 10 × 15 mesh alundum grains.

2. *Procedures.* Experimental procedures are given in detail in a previous paper[9]. The raw anthracite was first devolatilized in a N_2 stream at 950°C. The devolatilized anthracite was activated to the desired burnoff by continuously monitoring the amount of CO produced by gasification. A part of the activated sample was set aside for study and the remainder of the sample was used for subsequent runs at higher burnoffs.

---

[7] J. W. Hassler, *Proc. Anthracite Conf.*, Mineral Industries Experiment Station, The Pennsylvania State University, Bulletin No. 70, p. 1 (1957).

[8] J. W. Hassler, *Chem. Eng. Progr.* **52**, No. 12, 56 (1956).

[9] M. Kawahata and P. L. Walker, Jr., *Proc. Anthracite Conf.*, Mineral Industries Experiment Station, The Pennsylvania State University, Bulletin No. 75, pp. 63–78 (1961).

3. *Preliminary study on fluidization of anthracite.* Prior to activation runs, the flow rate of CO_2 which should be used to obtain optimum fluidization conditions for the different particle sizes of anthracite was determined in a glass reactor of dimensions identical to the Hastelloy-C reactor. This preliminary study on fluidization is also described in detail in a previous paper[9].

4. *Experimental design and conditions.* The experimental conditions covered the following ranges: (1) activation temperatures between 800 and 950°C, (2) burnoffs between 8 and 65%, and (3) particle sizes between 16 × 20 and 100 × 150 Tyler mesh. Three series of experiments, namely series A, B, and C were designed. In series A, the effect of activation temperature on pore structures was investigated in the lower and intermediate ranges of burnoff. In series B, the burnoff was extended to the higher range. In series C, the effect of particle size on the pore structure developed was investigated over the entire range of burnoff.

5. *Studies on Pore Structure.* The activated anthracites were characterized by the following physical data: surface area, helium and apparent densities, total open pore volumes, pore volume distributions, and micropore dimensions. A volumetric low temperature N_2 adsorption apparatus[10], a mercury porosimeter[11], and a helium density apparatus[12] were used.

III. EXPERIMENTAL RESULTS

A. *The Effect of Temperature on the Development of Pore Structure*

1. *Activation.* In the series A experiments, anthracite of 42 × 65 mesh size was activated at 4 temperatures between 800 and 950°C to burnoffs of 8, 16, 27, and 38%. In the series B experiments, based on the experimental results of series A, the degree of activation was extended to 53 and 65% at temperatures of 850 and 950°C. The flow rate of CO_2 was 0.037 ft³/min (S.T.P.). The starting weight of the devolatilized anthracite was 225 and 200 g in the series A and B experiments, respectively.

2. *Surface area.* Nitrogen adsorption isotherms at 78°K for all the samples were essentially of Type 1, indicating that monolayer adsorption predominated[13]. Surface areas could, therefore, be estimated closely using the Langmuir equation[14]. Calculated specific surface areas are listed in Table II.

TABLE II

Variation in Specific Surface Areas for 42 × 65 Mesh Activated Anthracites with Changes in Burnoff and Activation Temperature

Burnoff	Surface area, m²/g of anthracite for activation at			
%	800°C	850°C	900°C	950°C
nil	—	—	—	37
8	248	268	256	200
16	472	473	446	385
27	812	740	727	628
38	1033	1072	992	865
52	—	1450	—	1100
65	—	1890	—	1600

A variance analysis based on the F-ratio test was used to separate the effect of activation temperature from the effect of burnoff

[10] P. L. Walker, Jr., R. J. Foresti, Jr., and C. C. Wright, *Ind. Eng. Chem.* **45**, 1703 (1953).

[11] E. Raats, Ph.D. thesis, The Pennsylvania State University (1955).

[12] I. Geller, Ph.D. thesis, The Pennsylvania State University (1959).

[13] H. E. Ries, Jr., *Catalysis*, Reinhold, New York (1954), Vol. I, p. 1.

[14] For a closer approximation of surface area, the BET equation applicable where the number of adsorption layers is limited by the walls of pores having extremely small diameters should be used[15]. However, the use of this equation[16] is laborious and resulted in surface areas within 5% of those calculated using the Langmuir equation, for the anthracites activated to 8 and 38% burnoff at 900°C. Therefore, the Langmuir equation was used for the remainder of the samples.

[15] S. Brunauer, P. H. Emmett, and E. Teller, *J. Amer. Chem. Soc.* **60**, 309 (1945).

[16] L. G. Joyner, E. B. Weinberger, and C. W. Montgomery, *J. Amer. Chem. Soc.* **67**, 2182 (1945).

on the development of surface area. The estimated variance of these two factors was compared to the variance of the two-factor interactions to obtain F-ratios, using the data up to 38% burnoff. This F-ratio test revealed that the effect of temperature is not significant between 800 and 900°C, whereas the effect of burnoff is highly significant. At each temperature, the specific surface area increased linearly with burnoff. At activation temperatures of 900°C and below, the increase in area per unit of burnoff was greater than at 950°C.

Taking a unit weight of devolatilized anthracite as a basis, the variation of surface area with burnoff for activation temperatures of 850 and 950°C is calculated and shown in Fig. 1. The optimum burnoff

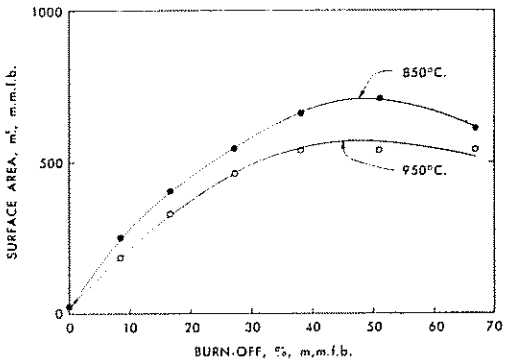

FIG. 1. Variation of surface area with burnoff for 42 × 65 mesh anthracite activated at 850 and 950°C. (Basis—a unit weight of devolatilized anthracite).

is *ca.* 50% for both temperatures; the specific surface areas at this burnoff are 1420 and 1130 m^2/g for activation temperatures of 850 and 950°C, respectively.

3. *Apparent and helium densities.* After devolatilization, anthracite may be considered to consist of a carbon and a mineral matter phase. Assuming the additivity of the volumes of these two phases, a negligible internal porosity in the mineral matter, and a mineral density of 2.7 g/cm^3,[17] the measured apparent and helium densities were converted to a mineral-matter-free basis. The calculated densities are listed in Table III and a typical variation of densities with burnoff is shown in Fig. 2.

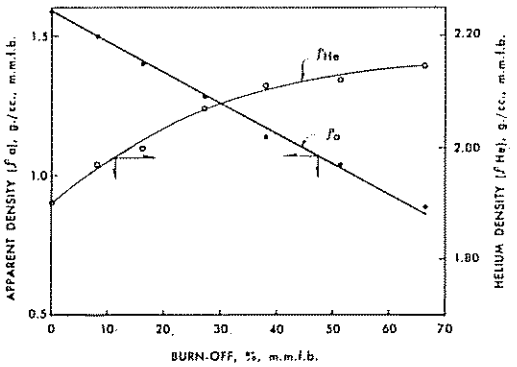

FIG. 2. Variation of apparent and helium densities with burnoff for 42 × 65 mesh anthracite activated at 850°C.

The apparent densities (ρ_a) decreased linearly with burnoff at all temperatures. The helium densities (ρ_{He}) increased with burnoff the rate of change decreasing as burno proceeded.

4. *Pore volume.* The specific, total pore volume, V_T, is calculated from the difference between the specific volumes given by the apparent and helium densities[18]. The specific pore volume, V_1, the volume in pores greater than 300 Å in diameter, was obtained directly from the porosimeter data. The specific pore volumes, V_T and V_1, are listed in Table III.

A variance analysis was made to separate the effect of temperature and burnoff on the

[17] A. M. Wandless and J. C. Macrae, *Fuel* (*London*) **13**, 4 (1934).

[18] It should be noted that this is actually the specific, total pore volume open to helium. The specific, total pore volume, open plus closed to helium, has not been considered in detail in this work. From X-ray diffraction measurements of the devolatilized anthracite[19], the true density is estimated to be 2.20 g/cm^3, or the specific, total pore volume, open plus closed, is 0.18 cm^3/g. This can be compared with the specific, total pore volume open to helium, 0.11 cm^3/g, which gives 39% closed porosity in the unactivated anthracite.

[19] M. A. Short, Ph.D. Thesis, The Pennsylvan State University (1961)

TABLE III

Variation in Densities and Pore Volumes of 42 × 65 Mesh Activated Anthracites with Changes in Burnoff and Activation Temperature

Burnoff %	Apparent density ρ_a, g/cm³	Helium density ρ_{He}, g/cm³	Specific, total pore volume, V_g cm³/g	Specific pore volume, V_1 ($D > 300$ Å), cm³/g
		Activated at 800°C		
8	1.51_0	1.95_7	0.151	0.006
16	1.42_4	1.99_8	0.203	0.007
27	1.28_4	2.07_3	0.302	0.013
38	1.17_6	2.10_6	0.392	0.020
		Activated at 850°C		
8	1.49_1	1.96_6	0.162	0.006
16	1.39_6	1.99_6	0.215	0.012
27	1.28_4	2.07_1	0.296	0.012
38	1.13_4	2.11_3	0.409	0.020
52	1.03_9	2.12_0	0.491	0.026
65	0.887	2.14_6	0.661	0.047
		Activated at 900°C		
8	1.49_1	1.95_3	0.159	0.005
16	1.41_5	2.01_1	0.210	0.010
27	1.27_5	2.04_6	0.296	0.016
38	1.15_4	2.11_2	0.393	0.019
		Activated at 950°C		
nil	1.58_5	1.90_3	0.108	0.003
8	1.49_9	1.99_6	0.161	0.007
16	1.41_8	2.00_7	0.207	0.009
27	1.29_7	2.05_3	0.283	0.015
38	1.17_2	2.09_1	0.375	0.018
52	1.07_6	2.07_5	0.447	0.042
65	0.91_0	2.11_0	0.625	0.055

variation of specific, total pore volume, using the data up to 38% burnoff. A variance analysis based on the F-ratio test showed that the effect of burnoff is highly significant, whereas the effect of activation temperature is not significant between 800 and 900°C. Taking a unit weight of devolatilized anthracite as a basis, the variation of total pore volume with burnoff is calculated and is shown in Fig. 3. The total pore volume goes through a maximum at *ca.* 43% burnoff for both temperatures. Specific, total pore volumes at this burnoff are 0.43 and 0.39 cm³/g for activation temperatures of 850 and 950°C, respectively.

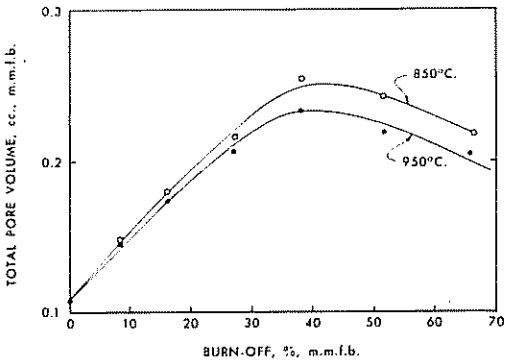

FIG. 3. Variation of total pore volume with burnoff for 42 × 65 mesh anthracite activated at 850 and 950°C. (Basis—a unit weight of devolatilized anthracite).

5. *Pore volume distribution.* Pore volume distributions for pores greater than 300 Å diameter were obtained by use of the mercury porosimeter. Pore volume distributions for pores smaller than 300 Å in diameter were obtained from N_2 adsorption isotherms by the method proposed by Cranston and

Inkley[20]. In their method, the increment of pore sizes for computation of the distribution was 20 Å from 300 to 100 Å, 10 Å down to 50 Å, 5 Å down to 20 Å and 2 Å down to 10 Å. Since V_T and V_1 are known, the specific pore volume in pores smaller than 10 Å in diameter may be calculated. Thus, complete cumulative pore volume distributions could be calculated. When they are plotted against diameter on logarithmic probability paper, three straight lines are approximated. A typical example of such a plot is shown in Fig. 4.

The pore volume which is available to N_2 at 78°K can be estimated from the adsorption isotherm data at a relative pressure of 1.0, assuming the normal liquid density for adsorbed N_2 molecules. This pore volume, V_N, is lower than the pore volume, V_T, for all of the samples, suggesting that $(V_T - V_N)$ is the pore volume in pores available to helium at room temperature but closed to N_2 at 78°K. Based on the molecular dimensions of these molecules, it appears that this volume is in pores of diameter less than 3 Å. Molecular sieve studies[21] also support this value for pore size. It is noted that the cumulative pore volume distribution plot when extrapolated to pore sizes smaller than 10 Å in diameter passes close to the point which is plotted assuming $(V_T - V_N)$ to be in pores less than 3 Å in diameter.

The cumulative pore distributions can be expressed mathematically by using normal distribution functions having three different sets of parameters for all the samples except those activated at 950°C beyond 27% burnoff. These three distributions are arbitrarily called the first, second and third distributions in the order of increasing pore diameters. For the samples which are exceptions, the first distribution function needs to be divided further into two functions. The normal distribution functions can be expressed as

$$dV = \frac{1}{\sqrt{(2\pi)}\sigma} \exp\left[-\frac{(y-\mu)^2}{2\sigma^2}\right] dy \qquad (1)$$

where y is ln D,

D is the diameter in Å,
V is the pore volume in %, and
μ and σ are the mean and variance of the distribution functions.

Since the first distributions are of prime importance in characterizing the adsorptive characteristics of activated carbons, on[1]·· their parameters are listed in Table I

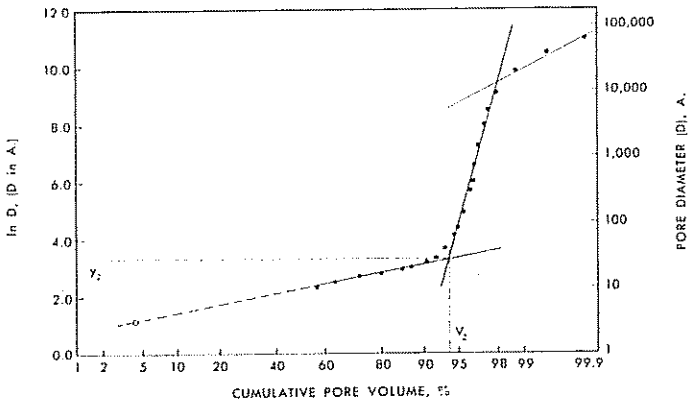

FIG. 4. Pore volume distribution of 42 × 65 mesh anthracite activated at 850°C to 38% burnoff.

[20] R. W. Cranston and F. A. Inkley, *Advances in Catalysis*, Academic Press, New York, Vol. IX (1957), pp. 143–154.

[21] D. W. Breck, W. G. Eversole, R. M. Milton, T. B. Reed, and T. L. Thomas, *J. Amer. Chem. Soc.* **78**, 5963 (1956).

TABLE IV

Variation in Parameters and Limiting Values of the First Pore Volume Distribution Function for 42 × 65 Mesh Activated Anthracites with Changes in Burnoff and Activation Temperature

Burnoff %	μ	σ	y_2[a]	D_2,[a] Å	V_2,[a] %
		Activated at 800°C			
8	1.52	1.42	3.3	28	90
16	2.02	0.90	3.4	30	93
27	2.18	0.64	3.2	25	93
38	2.33	0.70	3.4	30	92
		Activated at 850°C			
8	1.52	1.30	3.0	20	86
16	1.89	1.01	3.2	25	90
27	2.09	0.83	3.4	30	94
38	2.28	0.73	3.3	28	92
52	2.60	0.59	3.4	30	91
65	2.78	0.57	3.4	32	89
		Activated at 900°C			
8	1.35	1.32	3.4	30	94
16	1.85	1.09	3.3	27	94
27	2.07	0.86	3.3	27	92
38	2.35	0.83	3.6	38	93
		Activated at 950°C			
nil	−2.24	3.34	3.7	38	96
8	0.92	1.57	3.4	30	94
16	1.65	1.21	3.5	33	94
27	2.32	0.77	3.4	30	92
	2.35	1.47	2.3	—	49
38	2.55	0.74	3.7	38	93
	2.61	1.41	2.5	—	46
52	2.88	0.53	3.4	30	84
	3.12	1.39	2.8	—	39
65	3.05	0.49	3.5	35	86
	3.55	1.27	2.7	—	26

[a] Values at upper limit of first distribution function (see Fig. 4).

A typical variation of these parameters with burnoff is shown in Fig. 5 for the anthracite activated at 850°C. The mean of the distribution increases and the variance decreases with increasing burnoff.

It is noted that for all the activated anthracites, the first distribution accounts for approximately 92% of the total pore volume, and the upper limit of the distribution lies approximately at a pore diameter of 30 Å. The second and third distribution functions together account for approximately 8% of the total pore volume. The transition point between the second and the third distributions is approximately 10,000 Å for all samples.

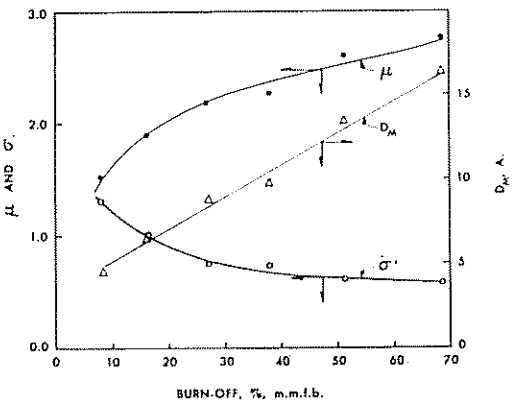

FIG. 5. Variation of parameters of the first pore volume distribution function with burnoff for 42 × 65 mesh anthracite activated at 850°C.

6. *Micropore dimensions.* Assuming eylindrical pores, the average pore diameter can be calculated from the pore volume distribution function. The general expression of the pore volume distribution is,

$$\mathrm{d}V/\mathrm{d}y = f(y) \tag{2}$$

For eylindrical pores having a diameter between D and $D + d(D)$, the following relationship holds:

$$(4V_T/D)\,\mathrm{d}V = \mathrm{d}A \tag{3}$$

Then, for pores having diameters between D_1 and D_2,

$$4V_T \int_{y_1}^{y_2} \frac{f(y)}{D}\,\mathrm{d}y = A \tag{4}$$

where A is the pore surface area. The average pore diameter may be defined as

$$\frac{1}{\bar{D}} \int_{y_1}^{y_2} f(y)\mathrm{d}y = \int_{y_1}^{y_2} \frac{f(y)}{D}\,\mathrm{d}y \tag{5}$$

Substituting Eq. (1) for $f(y)$,

$$\bar{D} = \exp\left(\frac{2\mu - \sigma^2}{2}\right) \times \frac{\displaystyle\int_{y_1}^{y_2} \exp\left[-\frac{(y-\mu)^2}{2\sigma^2}\right]\mathrm{d}y}{\displaystyle\int_{y_1}^{y_2} \exp\left[-\frac{[y-(\mu-\sigma^2)]^2}{2\sigma^2}\right]\mathrm{d}y} \tag{6}$$

Then, the pore surface area is

$$A = 4V_T \exp\left[-\frac{2\mu - \sigma^2}{2}\right] \times \int_{y_1}^{y_2} \frac{1}{\sqrt{(2\pi)}\sigma} \exp\left[-\frac{[y-(\mu-\sigma^2)]^2}{2\sigma^2}\right]\mathrm{d}y \tag{7}$$

Similarly, for eylindrical pores having diameters between D and $D + d(D)$,

$$V_T\mathrm{d}V = (\pi/4)D^2\mathrm{d}L \tag{8}$$

where L is the total pore length. For pores having diameter between D_1 and D_2,

$$(4V_T/\pi) \int_{y_1}^{y_2} \frac{f(y)}{D^2}\,\mathrm{d}y = L \tag{9}$$

The average square diameter may be defined as

$$\frac{1}{\bar{D}^2} \int_{y_1}^{y_2} f(y)\,\mathrm{d}y = \int_{y_1}^{y_2} \frac{f(y)}{D^2}\,\mathrm{d}y \tag{10}$$

Combining Eqs. (1), (9), and (10), the pore length is

$$L = \left(\frac{4V_T}{\pi}\right) \exp[-2(\mu - \sigma^2)] \times \int_{y_1}^{y_2} \frac{1}{\sqrt{(2\pi)}\sigma} \exp\left[-\frac{[y-(\mu-2\sigma^2)]^2}{2\sigma^2}\right]\mathrm{d}y \tag{11}$$

From Eqs. (6), (7) and (11), micropore dimensions (average pore diameter, pore surface area, and pore length) can be calculated for any pore size range.

These micropore dimensions calculated for pores over the range $3\ \text{Å} < D < 30\ \text{Å}$ are plotted against burnoff in Figs. 6–8.

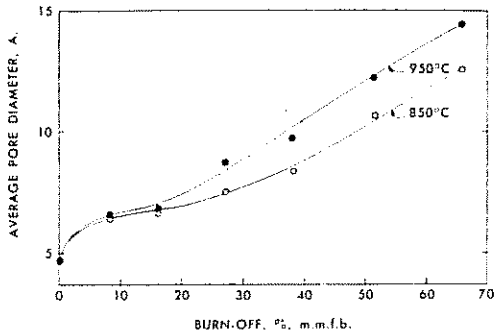

FIG. 6. Variation of average pore diameter over the range of $3\ \text{Å} < D < 30\ \text{Å}$ with burnoff for 42 × 65 mesh anthracite activated at 850 and 950°C.

They were calculated by taking a unit weight of devolatilized anthracite as a basis. Comparing Fig. 7 with Fig. 1, a significant difference between the areas calculated from the Langmuir equation and from the pore volume distribution function is observed, especially for the samples of lower burnoffs. These differences could be explained on the basis that the area assigned to a molecule of adsorbed N_2 in calculation using the Langmuir equation ($16.4\ \text{Å}^2$) is low in the case of extremely fine eylindrical pores.

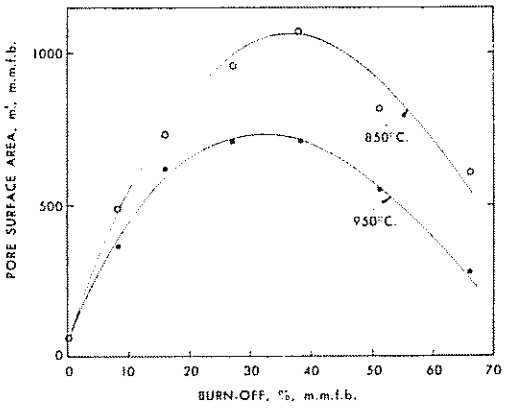

FIG. 7. Variation of pore surface area over the range $3\ \text{Å} < D < 30\ \text{Å}$ with burnoff for 42×65 mesh anthracite activated at 850 and 950°C. (Basis—a unit weight of devolatilized anthracite.)

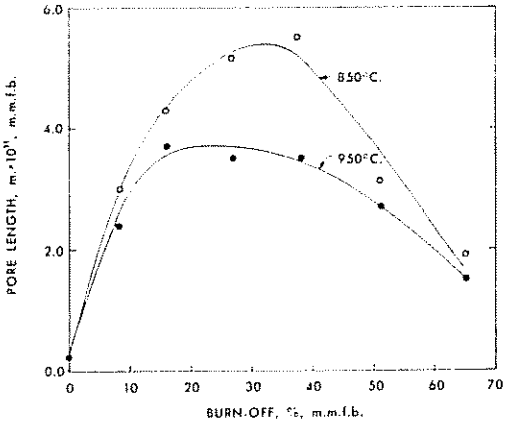

FIG. 8. Variation of pore length over the range $3\ \text{Å} < D < 30\ \text{Å}$ with burnoff for 42×65 mesh anthracite activated at 850 and 950°C. (Basis—a unit weight of devolatilized anthracite.)

B. *The Effect of Anthracite Particle Size on the Development of Pore Structure*

1. *Activation.* In order to investigate the effect of anthracite particle size on the development of pore structure upon activation, two additional particle sizes, 16×20 and 100×150 mesh (Tyler), were chosen. The activation temperature was fixed at 900°C, and the variation of the pore structure was investigated at burnoffs of 8, 22, 44 and *ca.* 65%. The flow rates of CO_2 were 0.02 and 0.18 ft³/min (S.T.P.) for 100×150 and 16×20 mesh sizes, respectively. These gas flow rates produced optimum fluidization conditions. The variations of pore structure with burnoff are presented in Figs. 9–11.

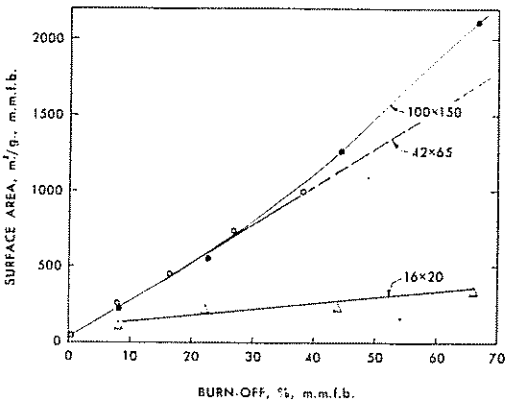

FIG. 9. Variation of specific surface area with burnoff for three particle sizes of anthracite activated at 900°C.

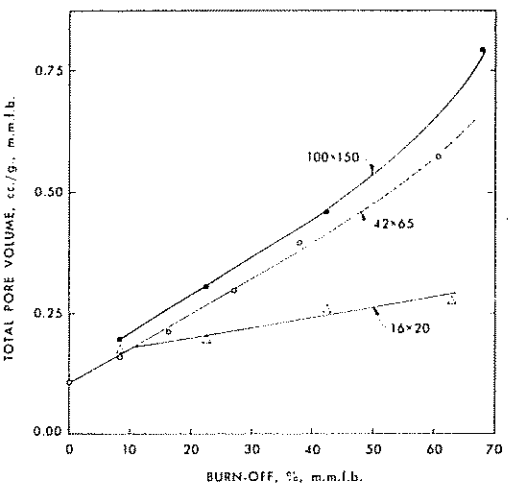

FIG. 10. Variation of specific total pore volume with burnoff for three particle sizes of anthracite activated at 900°C.

For the 42×65 mesh particle size, the variation of pore structure was extended beyond 38% by interpolation of the data found previously for activation at 850 and 950°C. This extension is shown in the figures by dotted lines.

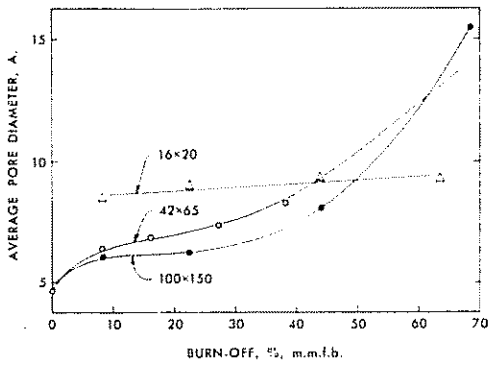

FIG. 11. Variation of average pore diameter over the range of $3\ \text{Å} < D < 30\ \text{Å}$ with burnoff for three particle sizes of anthracite activated at 900°C.

2. *Surface area.* As shown in Fig. 9, the specific surface area developed upon activation of the 16 × 20 mesh size fraction is considerably less than that developed upon activation of the two smaller particle size fractions. Up to about 25% burnoff, the development of specific surface area in the 100 × 150 and 42 × 65 mesh material is similar. At higher burnoffs there is some suggestion that area is developed more effectively in the 100 × 150 mesh size fraction.

3. *Densities and pore volume.* The helium densities for the 16 × 20 mesh fraction were essentially constant at about 1.91 g/cm³ over the entire range of burnoff. The apparent densities decreased linearly with burnoff for all the sizes, the decrease being more marked for the two smaller mesh fractions.

As shown in Fig. 10, the change of specific, total pore volume for the 100 × 150 mesh size is linear with burnoff up to *ca.* 44%; beyond this burnoff the increase is more rapid. Over the entire range of burnoff, the specific, total pore volume for this particle size is somewhat higher than for the 42 × 65 mesh size. The development of specific, total pore volume for the 16 × 20 mesh fraction is considerably less than that for the smaller sizes.

4. *Pore volume distribution and micropore dimensions.* In agreement with the results for the 42 × 65 mesh size, the first distribution function accounts for approximately 92% of the total pore volume for the 100 × 150 mesh size and it covers the range of pores less than *ca.* 30 Å in diameter. The first distribution function for the 16 × 20 mesh size fraction needed to be divided into two functions.

The variation of the average pore diameter over the range $3\ \text{Å} < D < 30\ \text{Å}$ with burnoff is shown for the three different particle size fractions in Fig. 11. For the 16 × 20 mesh size fraction, the average pore diameter is essentially constant at 9 Å over the entire range of burnoff investigated. For the two smaller particle size fractions, there is a substantial increase in average pore diameter with burnoff.

IV. DISCUSSION

Activated carbons which are suitable for vapor phase adsorption must contain a large internal surface area in micropores having diameters only somewhat larger than the molecular diameter of the vapor to be adsorbed. In this case, physical adsorption results, because of the attractive interaction energy between the adsorbate molecules and the surface atoms of the pores. It is generally agreed in the case of carbon, and most other solids, that the attractive interaction energy[22,23] arises from dispersion forces primarily, with the role of electrostatic polarization energy being small.

Anthracite is a suitable material for the production of activated carbons since it has a considerable pore volume in pores of and below molecular dimensions. It was suggested by Hirsch[3] that anthracite consists of graphitic lamellae of various diameters. The poor packing of these irregularly shaped

---

[22] M. M. Dubinin, *Industrial Carbon and Graphite Conference*, London (1958), p. 219.

[23] G. L. Kington and W. Laing, *Trans. Farada Soc.* **51**, 287 (1955).

lamellae is thought to produce pores. Bond[24] and Gregg and Pope[25] suggested that coal contains flat cavities some 40 to 60 Å across, connected with fine capillaries having a cross section very little in excess of the cross section of a nitrogen molecule. The production of activated carbons from anthracite may be considered to consist of the opening of sub-molecular pores and the enlargement of molecular pores to an extent such that an adsorbate will undergo a resulting, strong attractive interaction with the surface. If the pores are not developed sufficiently, the repulsive energy between the molecule to be adsorbed and the pore surface predominates, with adsorption being slow and/or negligible. If the pores are over-developed, the attractive interaction becomes small and adsorption at low relative pressures is negligible. Thus, the development of the pores is a result of the strategical removal of carbon atoms by gasification.

It is important that gasification occurs with a high degree of uniformity from the surface to the center of the particle, if an activated carbon having optimum properties is to be produced. If the reaction temperature is too high, or the particle size of carbon too large, Walker and co-workers[26] have shown that the carbon–carbon dioxide reaction proceeds non-uniformly through the particle, with some of the interior of the particle unreacted. This is called reaction Zone II[26]. At low over-all burnoffs, a large fraction of each particle will have undergone negligible reaction. At high over-all burnoffs, the exterior portion of each particle will have undergone too great a reaction resulting either in the complete disappearance of carbon or the leaving of a reacted shell which is too weak to withstand handling.

Walker and co-workers[26] showed that the dimensionless group

$$\left(\frac{R}{C_R D_{\text{eff}}}\right)\left(\frac{dn}{dt}\right) = \phi^2\eta \qquad (12)$$

where, R is the radius of the particle, cm,

CR is the reactant concentration, moles CO_2/cm^3,

D_{eff} is the effective diffusion coefficient, cm^2/sec, and

dn/dt is the over-all reaction rate per unit of geometric surface area of the particle, moles $CO_2/cm^2/sec$.

can be used to predict the uniformity of gasification, if retardation by products can be neglected.

For a first order reaction, if this group is less than 0.03, gasification should proceed uniformly through the particle. If this group is greater than 6.0, gasification should proceed in Zone II. The operation of an activator at a temperature sufficiently low to attain uniform gasification may be impractical economically, because of the low rate of throughput of activated carbon. In this case, the desirability of producing a uniformly activated product must be balanced against the desirability of a high throughput rate in order to select optimum operating conditions. These operating conditions will result in a value of $\phi^2\eta$ between 0.03 and 6.0.

It is of interest to calculate the values of $\phi^2\eta$ for some of the activating conditions used in this study. This calculation is made somewhat uncertain by the question of what value to use for D_{eff}. At present, studies are underway in this laboratory to measure D_{eff} on anthracites at activation temperatures. In lieu of appropriate experimental data at this time, the effective diffusivity is estimated from the following equations given by Wheeler[27]

[24] R. L. Bond, *Nature, London* **178**, 104 (1956).

[25] S. J. Gregg and M. I. Pope, *Fuel, London* **38**, 501 (1959).

[26] P. L. Walker, Jr., F. Rusinko, Jr. and L. G. Austin, *Advances in Catalysis*, Academic Press, New York (1959), vol. XI, p. 133.

[27] A. Wheeler, *Advances in Catalysis*, Academic Press, New York (1951), vol. III, pp. 249–327.

$$D = \tfrac{1}{3}\lambda v(1 - e^{-d/\lambda}) \quad (13)$$

$$D_{\text{eff}} = D(1/\gamma)(\epsilon) \quad (14)$$

where D is the diffusion coefficient in a single cylindrical pore, cm²/sec,
v is the mean molecular velocity, cm/sec,
λ is the mean free path, cm,
d is the pore diameter, cm,
γ is the tortuosity factor, and
ϵ is the surface porosity.

The surface porosity is physically the fraction of the particle boundary area corresponding to the cross sectional area of pores through which the reacting gas diffuses in from the exterior. Assuming that each pore has two openings to the external surface, ϵ is 1/3 of the appropriate volume porosity for a spherical particle. The tortuosity in Eq. (14) includes the degree of pore interconnections and pore constrictions, as well as the ratio of tortuous length to the straight path length.

In order to estimate the effective diffusivity from Eqs. (13) and (14), a pore structure model must be postulated, since D and ϵ depend upon the size and volume of pores through which the rate-controlling diffusional process takes place. It is recalled that for the majority of the activated anthracites, the pore volume distributions can be expressed mathematically by normal distribution functions having three different sets of parameters. These distributions are arbitrarily called the first, second and third distributions in the order of increasing pore diameter. It is proposed that pores in the second and third distributions, together, serve as main arteries for transport of the reacting gases from the exterior surface of the particles to the pores of the first distribution, which feed off the larger pores within the interior of the particle. Non-uniformity of activation in the anthracite particles (in the radial direction) then would be caused by a radial concentration gradient in the arterial pores.

The average pore diameter of the arterial pores can be calculated from the relationship $4\Sigma V/\Sigma A = d$, where ΣV and ΣA are the total pore volume and pore surface area, respectively, in the second and third distributions. The total pore surface area in the second and third distributions is computed by summing incremental areas calculated over each volume increment from the expression, $A = 4V/\bar{d}$, where $\bar{d}$ is the average pore diameter in the increment. This calculation gives an average pore diameter, d, of about 80 Å for the second and third distributions; this diameter is essentially constant between 8 and 38% burnoff. Using this diameter and a tortuosity of 20 from results of Hutcheon and co-workers on nuclear graphite[28], values of D_{eff} and then $\phi^2\eta$ were calculated for representative activation conditions and are given in Table V. For the representative runs considered in the calculations, these results predict that only those runs involving activation of the 16 × 20 mesh anthracite at 900°C would be expected to be in Zone II. The experimental results confirm this prediction, since the surface areas and pore volumes developed upon activation of the 16 × 20 mesh anthracite are markedly lower than those developed within the smaller mesh sizes of anthracite. It is clear, however, that even for the two smaller mesh sizes of anthracite, a decrease in activation temperature or particle size should result in some increase in pore development at comparable burnoffs. Such is seen to be the case from the experimental surface area and pore volume results.

During the activation of anthracite with CO_2, the following two processes can take place: (1) the formation of new pores by preferential removal of carbon atoms or the opening of new pores which existed

[28] J. M. Hutcheon and B. Longstaff, *Industrial Carbon and Graphite Conference*, London (1958) p. 259.

TABLE V

Summary of Diffusion-Control Criteria for Representative Activating Conditions

Activation conditions			D_{eff}	R	C_R	dn/dt	$\phi^2\eta$
Temp, °C	Burnoff, %	Particle size	cm^2/sec	cm	$mole/cm^3$	$mole/cm^2/sec$	
800	8	42 × 65	3.6×10^{-6}	1.35×10^{-2}	1.0×10^{-5}	0.46×10^{-9}	0.17
900	8	42 × 65	4.1	1.35	0.96	2.6	0.89
950	8	42 × 65	4.1	1.35	0.86	5.0	1.9
900	38	42 × 65	7.8	1.35	0.96	4.7	0.85
900	8	100 × 150	5.0	0.63	0.89	1.3	0.18
900	8	16 × 20	4.1	4.55	1.0	14.0	15.5
900	44	100 × 150	8.5	0.63	0.90	3.1	0.26
900	44	16 × 20	5.6	4.55	1.0	17.3	14.1

originally but which were closed, and (2) the enlargement of pores which existed or were newly opened. These two processes can be followed by references to Figs. 6–8. Consider, for example, the samples activated at 950°C. Both the pore surface area and pore length increase rapidly up to 16% burnoff. Beyond this burnoff, the increase in area is less, with the area being essentially constant between 27 and 40% burnoff. With further burnoff, the area decreases. Beyond 16% burnoff, the pore length gradually decreases and the average pore diameter starts to increase.

The general rules to be applied for the analysis of these micropore dimensions are as follows:

(1) Opening of new pores increases area and length. The effect on pore diameter depends on the pore sizes of newly opened pores.

(2) Enlargement of pores increases pore diameter and area but has no effect on pore length.

(3) Combination of adjacent pores, by gasifying away pore walls between them decreases the area and length greatly.

(4) Transformation of some pores to the larger pore size range by enlargement decreases area and length, but this decrease will be cancelled, at least partially, by enlargement of pores in the smaller diameter range of the distribution.

By applying these general rules to the 950°C data summarized above, it is concluded that the formation of new pores and enlargement of pores occur simultaneously, although during the initial stages of burnoff the opening of new pores predominates. At a certain stage of burnoff, the enlargement of pores exceeds the opening of new pores. This transition is estimated to take place at 16% burnoff for activation at 950°C. By similar reasoning, this transition is estimated to occur at 27% burnoff for activation at 850°C.

The authors wish to thank the Commonwealth of Pennsylvania under their continuing coal research program for supporting this study.